




## RESEARCH ARTICLE

WILEY

# Perturbation and numerical solutions of non-Newtonian fluid bounded within in a porous channel: Applications of pseudo-spectral collocation method

Mubbashar Nazeer<sup>1</sup>  | Fayyaz Ahmad<sup>2</sup>  | Waqas Ali<sup>3</sup> | Muhammad Ijaz Khan<sup>4</sup>  | Adila Saleem<sup>5</sup> | Zubair Khaliq<sup>6</sup> | Seifedine Kadry<sup>7</sup> | Yu-Ming Chu<sup>8,9</sup>

<sup>1</sup>Department of Mathematics, Institute of Arts and Science, Government College University Faisalabad, Faisalabad, Pakistan

<sup>2</sup>Department of Applied Sciences, National Textile University, Faisalabad, Pakistan

<sup>3</sup>Chair of Production Technology, Faculty of Engineering Technology, University of Twente, Twente, The Netherlands

<sup>4</sup>Department of Mathematics and Statistics I–14, Riphah International University, Islamabad, Pakistan

<sup>5</sup>Department of Mathematics, Riphah International University Faisalabad, Faisalabad, Pakistan

<sup>6</sup>Department of Polymer Engineering, National Textile University, Faisalabad, Pakistan

<sup>7</sup>Department of Mathematics and Computer Science, Beirut Arab University, Beirut, Lebanon

<sup>8</sup>Department of Mathematics, Huzhou University, Huzhou, P.R. China

<sup>9</sup>Hunan Provincial Key Laboratory of Mathematical Modeling and Analysis in Engineering, Changsha University of Science & Technology, Changsha, P.R. China

## Correspondence

Yu-Ming Chu, Department of Mathematics, Huzhou University, Huzhou 313000, P.R. China.  
Email: chuyuming@zjhu.edu.cn

## Funding information

National Natural Science Foundation of China, Grant/Award Numbers: 11601485, 11626101, 11701176, 61673169, 11871202, 11971142.

## Abstract

In the current study, the effects of fluidic parameters with entropy generation properties on velocity, temperature, and entropy numbers of non-Newtonian fluid flowing through the porous channel are investigated. The complex system of fluid equations is handled with analytically and numerically. The first-order perturbation expansion is employed on both velocity and temperature to obtain the approximate analytical solution. A comparison of the analytical solution is made with numerical results that are obtained by discretizing the system of boundary value problems. The pseudo-spectral collocation method was used for the discretization, and the Newton method was to get the solutions to the complex differential equations. In the Newton method, the finite difference approximation of Jacobian is utilized. The pseudo-spectral solutions are in good agreement with the analytical findings. The order of accuracy in temperature and velocity profiles is of order  $10^{-6}$  which will be compared in the future with the experimental results of given non-Newtonian fluid.

## KEYWORDS

Bejan and entropy numbers, Eyring–Powell fluid, perturbation method, porous channel, pseudo-spectral collocation method

## 1 | INTRODUCTION

In view of ever-increasing applications of non-Newtonian fluids in biochemical and process engineering, the importance of such fluids, specifically in the research field, has been enlarged from the last few decades. Non-Newtonian fluids indicate significant performance in boiling, polymers, plastic foam processing, coating, plasma, and slurries [1–13]. Many researchers focused on non-Newtonian fluid while considering various geometries. Some of the relevant literature is discussed in the following paragraphs.

A few essential investigations about non-Newtonian properties of fluids have been performed in these papers, which motivate the researchers towards the study of such complex fluids. Ali et al. [14, 15] have employed the finite element method to calculate the porous, and magnetic effects on velocity and temperature distributions of the non-Newtonian fluids. Kefayati [16] used the Lattice Boltzmann method to analyze the entropy generation in a power-law fluid through an inclined enclosure. They concluded that the mass transfer enhances against the Soret parameter. In another study [17], he considered the Bingham fluid inside an open conduit to highlight the importance of free convection flow. Sheremet and Pop [18] investigated the water-based nanofluid of steady laminar mixed convection in a lid-driven cavity. They described the effects of pertinent parameters, namely, Reynolds, Prandtl, and Lewis numbers on local Sherwood and local Nusselt numbers. They also compared their results with previously published data. The work on heat transfer enhancement of nanofluids is further extended by Turkyilmazoglu [19]. He studied the heat transfer under the effects of limited velocity slips in circular pipes. He used the single-phase nanofluid model to calculate the exact solution of the problem. He also discussed the slip effects on different nanofluids with the solution for temperature and velocity profiles. Sheremet et al. [20] reported the magnetic effects on the cavity flow problems by using the numerical scheme and highlighted the increment of heat transfer rate via the viscosity parameter. Elniel et al. [21] investigated the magnetic field effects on MHD Powell–Eyring fluid near the accelerated plates with constant properties. Adomian decomposition method is used to solve the nonlinear system of equations. The analysis of heat and mass transmission influences for the unsteady flow of EP non-Newtonian fluid passing through the stretching sheet performed by Krishna et al. [22]. Their results showed that the heat transfer decreases, and mass transfer increase by increasing the chemical reaction parameters. The properties of entropy generation in the magnetohydrodynamic flow of Eyring–Powell fluid over a stretching surface are inspected by Alharbi et al. [23]. They discussed the effect of the heat source and thermal radiation on fluid flow. The stagnation point flow of EP non-Newtonian fluid above the stretching sheet was evaluated by Javed et al. [24]. They obtained the numerical solution by applying the Keller box method and the effect of material parameters on the velocity distribution and skin-friction coefficient described in detail. The heat flux and magnetic field characteristics of EP nanofluid flowing above a sheet were examined by Malik et al. [25]. The shooting method was used to calculate the numerical solution of the problem. Kumar et al. [26] evaluated the 3D mixed convection flow of EP nanofluid under the effect of flow and heat transfer. The results revealed mixed convection parameter diminishes the mass concentration and temperature fields for higher values. Some relevant investigations related to Eyring–Powell fluid can be mentioned in these studies [6, 27–31].

In the previous investigation, Khan et al. [32] discussed the Eyring–Powell fluid with entropy generation in the porous horizontal channel. They used the semi-analytical scheme to handle the nonlinear complex fluid equations and validated their solution with the shooting method. The analytical expressions of velocity, temperature, and entropy number were missing in their study. Furthermore, they did not provide the error magnitude in velocity and temperature profile, which has significant importance while considering such a problem. The ranges of fluidic parameters were also missing in their study.

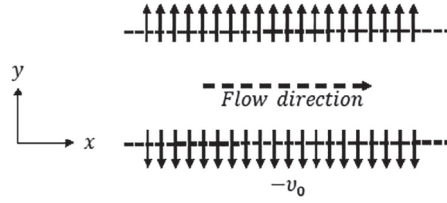


FIGURE 1 Geometric depiction of the porous flow channel

The objectives of our investigation are:

- (i) Obtain the analytical expressions of velocity, temperature, and entropy number.
- (ii) Provide the ranges of fluidic parameters used.
- (iii) Compare the analytical solution with a numerical solution.

## 2 | PROBLEM FORMULATION

The flow of Eyring–Powell fluid in the horizontal parallel plates is considered, as illustrated in Figure 1. Cartesian coordinate system is taken in which  $\hat{x}$  and  $\hat{y}$  directions are parallel and perpendicular to the channel, respectively.

The extra shear tensor for the present investigation is given as [1]:

$$\hat{\tau}_{\hat{xy}} = \mu \frac{\partial \hat{u}}{\partial \hat{y}} + \frac{1}{k_1} \text{Sinh}^{-1} \left( \frac{1}{k_2} \frac{\partial \hat{u}}{\partial \hat{y}} \right). \quad (1)$$

By using the expansion, we get

$$\text{Sinh}^{-1} \left( \frac{1}{k_2} \frac{\partial \hat{u}}{\partial \hat{y}} \right) = \frac{1}{k_2} \frac{\partial \hat{u}}{\partial \hat{y}} - \frac{1}{6} \left( \frac{1}{k_2} \frac{\partial \hat{u}}{\partial \hat{y}} \right)^3, \quad \left| \frac{1}{k_2} \frac{\partial \hat{u}}{\partial \hat{y}} \right| \ll 1. \quad (2)$$

The important flow equations are given by

$$\frac{\partial \hat{u}}{\partial \hat{x}} = 0, \quad (3)$$

$$-\hat{v}_0 \frac{\partial \hat{u}}{\partial \hat{y}} = -\frac{1}{\rho} \frac{\partial \hat{p}}{\partial \hat{x}} + \frac{1}{\rho} \frac{\partial}{\partial \hat{y}} \hat{\tau}_{\hat{xy}}, \quad (4)$$

$$\rho \hat{C}_{\hat{p}} \left( -\hat{v}_0 \frac{\partial \hat{\theta}}{\partial \hat{y}} \right) = \kappa \frac{\partial^2 \hat{\theta}}{\partial \hat{y}^2} + \hat{\tau}_{\hat{xy}} \frac{\partial \hat{u}}{\partial \hat{y}}, \quad (5)$$

where  $\mu$ , dynamic viscosity of fluid;  $k_1, k_2$ , material parameters;  $\rho$ , fluid density;  $\hat{v}$ , kinematic viscosity;  $\hat{C}_{\hat{p}}$ , specific heat;  $\hat{p}, k$ , pressure and thermal conductivity, respectively.

By substituting Equation (1) into Equations (4) and (5), we have the following momentum and energy equations in dimensional form:

$$-\hat{v}_0 \frac{\partial \hat{u}}{\partial \hat{y}} = -\frac{1}{\rho} \frac{\partial \hat{p}}{\partial \hat{x}} + \left( \hat{v} + \frac{1}{\rho k_1 k_2} \right) \frac{\partial^2 \hat{u}}{\partial \hat{y}^2} - \frac{1}{2 \rho k_1 k_2^3} \left( \frac{\partial \hat{u}}{\partial \hat{y}} \right)^2 \frac{\partial^2 \hat{u}}{\partial \hat{y}^2}, \quad (6)$$

$$\rho \hat{C}_{\hat{p}} \left( -\hat{v}_0 \frac{\partial \hat{\theta}}{\partial \hat{y}} \right) = k \frac{\partial^2 \hat{\theta}}{\partial \hat{y}^2} + \left( \mu + \frac{1}{k_1 k_2} \right) \left( \frac{\partial \hat{u}}{\partial \hat{y}} \right)^2 - \frac{1}{6 k_1 k_2^3} \left( \frac{\partial \hat{u}}{\partial \hat{y}} \right)^4. \quad (7)$$

To compute the constants for the solution of Equations (6) and (7), two boundary conditions are required. These boundary conditions at the lower and upper boundary of the channel are:

$$\begin{aligned} \hat{u}(0) &= 0, & \hat{u}(\hat{h}) &= 0, \\ \hat{\theta}(0) &= \hat{\theta}_0, & \hat{\theta}(\hat{h}) &= \hat{\theta}_{\hat{h}}. \end{aligned} \quad (8)$$

To transform Equations (6) and (7) into dimensionless form, we introduce the following dimensionless variables:

$$\eta = \frac{\hat{y}}{\hat{h}}, \quad u_1 = \frac{\hat{u}}{\hat{v}_0}, \quad \theta = \frac{\hat{\theta} - \hat{\theta}_0}{\hat{\theta}_{\hat{h}} - \hat{\theta}_0}. \quad (9)$$

By using the above mentioned non-dimensional quantities into Equations (6) and (7), we have the following dimensionless momentum and energy equations:

$$(1 + S) \frac{\partial^2 u_1}{\partial \eta^2} + Re \frac{\partial u_1}{\partial \eta} - K \frac{\partial^2 u_1}{\partial \eta^2} \left( \frac{\partial u_1}{\partial \eta} \right)^2 = -P, \quad (10)$$

$$\frac{\partial^2 \theta}{\partial \eta^2} + Pe \frac{\partial \theta}{\partial \eta} + Br \left( (1 + S) \left( \frac{\partial u_1}{\partial \eta} \right)^2 - \frac{b}{6} \left( \frac{\partial u_1}{\partial \eta} \right)^4 \right) = 0. \quad (11)$$

Wherein the above equations,

$$\begin{aligned} Re &= \frac{\hat{v}_0 \hat{h}}{\hat{\nu}}, & Pe &= \frac{\hat{v}_0 \hat{h} \rho \hat{C}_p}{k}, & P &= \frac{\hat{h}^2}{\hat{v}_0 \hat{\nu} \rho} \left( -\frac{\partial \hat{p}}{\partial \hat{x}} \right), \\ Br &= \frac{\mu \hat{v}_0^2}{k(\hat{\theta}_{\hat{h}} - \hat{\theta}_0) \hat{h}^2}, & S &= \frac{1}{\mu k_1 k_2}, & K &= \frac{S \hat{v}_0^2}{2k_2 \hat{h}^2}, & b &= \frac{\hat{v}_0^2}{\mu k_1 k_2 \hat{h}^2}. \end{aligned} \quad (12)$$

In the above boundary value problem  $Re$ ,  $Br$ , and  $Pe$  are the Reynolds, Brinkman, and Peclet numbers respectively,  $P$  is the pressure parameter,  $S$ ,  $K$ , and  $b$  are the material parameters of an Eyring–Powell fluid,  $u_1$  is the velocity component,  $\theta$  is the temperature of the fluid.

Next, by using dimensionless quantities in Equation (8), boundary conditions in dimensionless form become:

$$\begin{aligned} u_1(0) &= 0, & u_1(1) &= 0, \\ \theta(0) &= 0, & \theta(1) &= 1. \end{aligned} \quad (13)$$

### 3 | PERTURBATION METHOD

To obtain the approximate analytical solution of equation (10) and (11), we use the perturbation technique. For this, we consider the following relation:

$$u_1 = U_0 + \epsilon U_1 + O(\epsilon^2), \theta = \theta_0 + \epsilon \theta_1 + O(\epsilon^2), K = \epsilon \sigma, Br = \epsilon b_1,$$

$$\text{and setting } \Gamma = (1 + S) \quad (14)$$

where  $\epsilon(0 < \epsilon \ll 1)$  is a known perturbation parameter. Comparing the coefficient of order  $\epsilon^0$ , from Equations (10) and (13a) we obtain

Order  $\epsilon^0$ :

$$\Gamma \frac{\partial^2 U_0}{\partial \eta^2} + Re \frac{\partial U_0}{\partial \eta} + P = 0, \quad (15)$$

$$U_0(0) = 0, \quad U_0(1) = 0. \tag{16}$$

Solving Equation (15), we obtain the general solution of Equation (15) is:

$$U_0 = -\frac{P\eta}{Re} - \left( \frac{\Gamma e^{-\frac{Re\eta}{\Gamma}}}{Re} \right) c_1 + c_2. \tag{17}$$

Using the boundary conditions (15) in Equation (17), the values of arbitrary constant  $c_1$  and  $c_2$  are:

$$c_1 = \frac{e^{\frac{Re}{\Gamma}} P}{\Gamma \left( -1 + e^{\frac{Re}{\Gamma}} \right)}, \quad c_2 = \frac{e^{\frac{Re}{\Gamma}} P}{\left( -1 + e^{\frac{Re}{\Gamma}} \right) Re}. \tag{18}$$

With the help of the above integration constants  $c_1$  and  $c_2$ , Equation (17) becomes

$$U_0 = \lambda_0 \eta + \lambda_1 \left( 1 - e^{-\frac{Re\eta}{\Gamma}} \right). \tag{19}$$

System of the order of  $\epsilon$ ,

Order  $\epsilon^1$ :

$$\Gamma \frac{\partial^2 U_1}{\partial \eta^2} + Re \frac{\partial U_1}{\partial \eta} - \sigma \left( \frac{\partial U_0}{\partial \eta} \right)^2 \frac{\partial^2 U_0}{\partial \eta^2} = 0, \tag{20}$$

$$U_1(0) = 0, \quad U_1(1) = 0. \tag{21}$$

Using Equation (19) into Equation (20), we get the general solution of a system of  $O(\epsilon^1)$  as:

$$U_1 = c_4 - \frac{e^{-\frac{Re\eta}{\Gamma}} \Gamma c_3}{Re} + \sigma \left( \begin{array}{l} \frac{e^{-\frac{Re\eta}{\Gamma}} \lambda_0^2 \lambda_1}{\Gamma} + \frac{e^{-\frac{Re\eta}{\Gamma}} Re \eta \lambda_0^2 \lambda_1}{\Gamma^2} \\ - \frac{e^{-\frac{2Re\eta}{\Gamma}} Re \lambda_0 \lambda_1^2}{\Gamma^2} - \frac{e^{-\frac{3Re\eta}{\Gamma}} Re^2 \lambda_1^3}{6\Gamma^3} \eta \end{array} \right). \tag{22}$$

The values of  $c_3$  and  $c_4$  are obtained by employing the boundary condition which is given in Equation (21) as:

$$c_3 = \frac{\sigma Re \lambda_1 e^{-\frac{2Re}{\Gamma}}}{6\Gamma^4 \left( -1 + e^{\frac{Re}{\Gamma}} \right)} \left( -6\Gamma^2 \lambda_0^2 e^{\frac{2Re}{\Gamma}} + 6\Gamma^2 \lambda_0^2 e^{\frac{3Re}{\Gamma}} - 6\Gamma Re \lambda_0^2 e^{\frac{2Re}{\Gamma}} + 6\Gamma Re \lambda_0 \lambda_1 e^{\frac{Re}{\Gamma}} - 6\Gamma Re \lambda_0 \lambda_1 e^{\frac{3Re}{\Gamma}} + Re^2 \lambda_1^2 - Re^2 \lambda_1^2 e^{\frac{3Re}{\Gamma}} \right),$$

$$c_4 = -\frac{\sigma Re \lambda_1 e^{-\frac{2Re}{\Gamma}}}{6\Gamma^3 \left( -1 + e^{\frac{Re}{\Gamma}} \right)} \left( 6\Gamma \lambda_0^2 e^{\frac{2Re}{\Gamma}} - 6\Gamma \lambda_0 \lambda_1 e^{\frac{Re}{\Gamma}} + 6\Gamma \lambda_0 \lambda_1 e^{\frac{2Re}{\Gamma}} + Re \lambda_1^2 e^{\frac{2Re}{\Gamma}} \right). \tag{23}$$

With the help of the values of  $c_3$  and  $c_4$ , Equation (22) can also be defined as

$$U_1 = \sigma \left( \begin{array}{l} \lambda_2 + \lambda_3 \left( e^{-\frac{Re\eta}{\Gamma}} - \eta e^{-\frac{Re\eta}{\Gamma}} + \eta e^{\frac{Re(1-\eta)}{\Gamma}} \right) + \lambda_4 \left( e^{-\frac{2Re\eta}{\Gamma}} - e^{\frac{Re(1-2\eta)}{\Gamma}} - e^{-\frac{Re(1+\eta)}{\Gamma}} + e^{\frac{Re(1-\eta)}{\Gamma}} \right) \\ + \lambda_5 \left( e^{-\frac{3Re\eta}{\Gamma}} - e^{\frac{Re(1-3\eta)}{\Gamma}} - e^{-\frac{Re(2+\eta)}{\Gamma}} + e^{\frac{Re(1-\eta)}{\Gamma}} \right) \end{array} \right). \tag{24}$$

The expression of velocity in terms of original parameters is defined by

$$u_1 = \lambda_0 \eta + \lambda_1 \left( 1 - e^{-\frac{Re\eta}{\Gamma}} \right) + K \left( \begin{array}{l} \lambda_2 + \lambda_3 \left( e^{-\frac{Re\eta}{\Gamma}} - \eta e^{-\frac{Re\eta}{\Gamma}} + \eta e^{\frac{Re(1-\eta)}{\Gamma}} \right) + \\ \lambda_4 \left( e^{-\frac{2Re\eta}{\Gamma}} - e^{\frac{Re(1-2\eta)}{\Gamma}} - e^{-\frac{Re(1+\eta)}{\Gamma}} + e^{\frac{Re(1-\eta)}{\Gamma}} \right) \\ + \lambda_5 \left( e^{-\frac{3Re\eta}{\Gamma}} - e^{\frac{Re(1-3\eta)}{\Gamma}} - e^{-\frac{Re(2+\eta)}{\Gamma}} + e^{\frac{Re(1-\eta)}{\Gamma}} \right) \end{array} \right). \tag{25}$$

Order  $\epsilon^0$ :

$$\frac{\partial^2 \theta_0}{\partial \eta^2} + Pe \frac{\partial \theta_0}{\partial \eta} = 0, \tag{26}$$

$$\theta_0(0) = 0, \quad \theta_0(1) = 1. \quad (27)$$

To obtain the general solution of the order of one, solving Equation (26) and we get:

$$\theta_0 = -\frac{e^{-Pe\eta}c_5}{Pe} + c_6, \quad (28)$$

The constants of integration  $c_5$  and  $c_6$  are obtained by using the boundary condition which is defined in Equation (27):

$$c_5 = \frac{e^{Pe}Pe}{-1 + e^{Pe}}, \quad c_6 = \frac{e^{Pe}}{-1 + e^{Pe}}. \quad (29)$$

$$\theta_0 = \chi_0(1 - e^{-Pe\eta}), \quad (30)$$

Order  $\epsilon^1$ :

$$\frac{\partial^2 \theta_1}{\partial \eta^2} + Pe \frac{\partial \theta_1}{\partial \eta} + b_1 \Gamma \left( \frac{\partial U_0}{\partial \eta} \right)^2 - \frac{bb_1}{6} \left( \frac{\partial U_0}{\partial \eta} \right)^4 = 0, \quad (31)$$

$$\theta_1(0) = 0, \quad \theta_1(1) = 0. \quad (32)$$

To find the solution of Equation (31), the values of  $U_0$  which is given in Equation (19) are used to obtain the general solution and solution of  $\theta_1$  is:

$$\theta_1 = c_8 + \chi_1 e^{-Pe\eta} c_7 + b_1 \left( \chi_2 \eta + \chi_3 e^{-\frac{Re\eta}{\Gamma}} + \chi_4 e^{-\frac{2Re\eta}{\Gamma}} + \chi_5 e^{-\frac{3Re\eta}{\Gamma}} + \chi_6 e^{-\frac{4Re\eta}{\Gamma}} \right). \quad (33)$$

The values of the constant of integration  $c_7$  and  $c_8$  are obtained by using Equation (32) and that values are:

$$c_7 = -\frac{-b_1(\chi_3 + \chi_4 + \chi_5 + \chi_6) + b_1 \left( \chi_2 + e^{-\frac{Re}{\Gamma}} \chi_3 + e^{-\frac{2Re}{\Gamma}} \chi_4 + e^{-\frac{3Re}{\Gamma}} \chi_5 + e^{-\frac{4Re}{\Gamma}} \chi_6 \right)}{-\chi_1 + e^{-Pe} \chi_1},$$

$$c_8 = -\frac{b_1 e^{-\frac{4Re}{\Gamma}} \left( e^{Pe + \frac{4Re}{\Gamma}} \chi_2 - e^{\frac{4Re}{\Gamma}} \chi_3 + e^{Pe + \frac{3Re}{\Gamma}} \chi_3 - e^{\frac{4Re}{\Gamma}} \chi_4 + e^{Pe + \frac{2Re}{\Gamma}} \chi_4 \right)}{-e^{\frac{4Re}{\Gamma}} \chi_5 + e^{Pe + \frac{Re}{\Gamma}} \chi_5 + e^{Pe} \chi_6 - e^{\frac{4Re}{\Gamma}} \chi_6}.$$

With the help of the above constants we get

$$\theta_1 = b_1 \left( \chi_2 \eta + \chi_3 e^{-\frac{Re\eta}{\Gamma}} + \chi_4 e^{-\frac{2Re\eta}{\Gamma}} + \chi_5 e^{-\frac{3Re\eta}{\Gamma}} + \chi_6 e^{-\frac{4Re\eta}{\Gamma}} + \chi_7 e^{-Pe\eta} + \chi_8 \right). \quad (35)$$

The temperature in terms of the original parameter is defined as

$$\theta = \chi_0(1 - e^{-Pe\eta}) + Br \left( \chi_2 \eta + \chi_3 e^{-\frac{Re\eta}{\Gamma}} + \chi_4 e^{-\frac{2Re\eta}{\Gamma}} + \chi_5 e^{-\frac{3Re\eta}{\Gamma}} + \chi_6 e^{-\frac{4Re\eta}{\Gamma}} + \chi_7 e^{-Pe\eta} + \chi_8 \right). \quad (36)$$

#### 4 | ENTROPY GENERATION

To evaluate the entropy generation, we will use the following expression [32]

$$N_s = \left( \frac{d\theta}{d\eta} \right)^2 + \frac{Br}{\Omega} \left( \Gamma - \frac{b}{6} \left( \frac{du_1}{d\eta} \right)^2 \right) \left( \frac{du_1}{d\eta} \right)^2. \quad (37)$$

In the above Equation (37), the first term arises due to heat generation and which can be written as  $Ns_1$ , whereas the second term appears due to viscous dissipation and can be written as  $Ns_2$ , that is,

$$Ns_1 = \left(\frac{d\theta}{d\eta}\right)^2 \quad \text{and} \quad Ns_2 = \frac{Br}{\Omega} \left( \Gamma \left(\frac{du_1}{d\eta}\right)^2 - \frac{b}{6} \left(\frac{du_1}{d\eta}\right)^4 \right). \tag{38}$$

Using the analytical expressions of velocity and temperature profiles given in Equations (25) and (36), respectively into Equation (37) to obtain the final form of the entropy generation numbers, which is given by:

$$Ns = \left( e^{-Pe\eta} \chi_8 + Br \left( \chi_2 + e^{-\frac{Re\eta}{\Gamma}} \chi_9 + e^{-\frac{2Re\eta}{\Gamma}} \chi_{10} + e^{-\frac{3Re\eta}{\Gamma}} \chi_{11} + e^{-\frac{4Re\eta}{\Gamma}} \chi_{12} + e^{-Pe\eta} \chi_{13} \right) \right)^2 + \frac{Br}{\Omega} \left\{ \Gamma \left( \lambda_0 + e^{-\frac{Re\eta}{\Gamma}} \lambda_6 + K \left( \lambda_3 \left( -e^{-\frac{Re\eta}{\Gamma}} + e^{\frac{Re(1-\eta)}{\Gamma}} \right) - \lambda_7 \left( e^{-\frac{Re\eta}{\Gamma}} - e^{-\frac{Re\eta}{\Gamma}} \eta + e^{\frac{Re(1-\eta)}{\Gamma}} \eta \right) - \lambda_8 \left( 2e^{-\frac{2Re\eta}{\Gamma}} - e^{-\frac{Re(1+\eta)}{\Gamma}} - 2e^{\frac{Re(1-2\eta)}{\Gamma}} + e^{\frac{Re(1-\eta)}{\Gamma}} \right) - \lambda_9 \left( 3e^{-\frac{3Re\eta}{\Gamma}} - e^{-\frac{Re(2+\eta)}{\Gamma}} - 3e^{\frac{Re(1-3\eta)}{\Gamma}} + e^{\frac{Re(1-\eta)}{\Gamma}} \right) \right) \right) \right\} - \frac{1}{6} b \left\{ \lambda_0 + e^{-\frac{Re\eta}{\Gamma}} \lambda_6 + K \left( \lambda_3 \left( -e^{-\frac{Re\eta}{\Gamma}} + e^{\frac{Re(1-\eta)}{\Gamma}} \right) - \lambda_7 \left( e^{-\frac{Re\eta}{\Gamma}} - e^{-\frac{Re\eta}{\Gamma}} \eta + e^{\frac{Re(1-\eta)}{\Gamma}} \eta \right) - \lambda_8 \left( 2e^{-\frac{2Re\eta}{\Gamma}} - e^{-\frac{Re(1+\eta)}{\Gamma}} - 2e^{\frac{Re(1-2\eta)}{\Gamma}} + e^{\frac{Re(1-\eta)}{\Gamma}} \right) - \lambda_9 \left( 3e^{-\frac{3Re\eta}{\Gamma}} - e^{-\frac{Re(2+\eta)}{\Gamma}} - 3e^{\frac{Re(1-3\eta)}{\Gamma}} + e^{\frac{Re(1-\eta)}{\Gamma}} \right) \right) \right) \right\}. \tag{39}$$

To calculate the Bejan number, we have

$$Be = Ns_1 / (Ns_1 + Ns_2), \tag{40}$$

or

$$Be = 1 / (1 + \phi). \tag{41}$$

### 5 | PSEUDO-SPECTRAL COLLOCATION METHOD

The coupled system of nonlinear equations is discretized by using the pseudo-spectral collocation method [33]. It is well known that the pseudo-spectral collocation method offers high accuracy in the approximation of derivatives. Equations (10) and (11) are nonlinear and represent second-order boundary value problems. The domain of our problems is [0,1] and usually, the matrix operators in pseudo-spectral collocation method to approximate the derivatives are defined over the domain [-1,1] and there is a transformation  $\Gamma$  from [-1,1] to [0,1], that is,

$$\Gamma = [-1, 1] \rightarrow [0, 1] : \Gamma(r) = 0.5 (r + 1). \tag{42}$$

We discretize the domain of our problem [0,1] and introduce  $n$ -grid points:

$$\eta_i = (i - 1)h, \text{ for } i = 1, 2, 3, \dots, n.$$

where  $h = \frac{1}{n-1}$ . If we denote the differentiation pseudo-spectral collocation matrix by  $\bar{\mathbf{D}}$  then matrix operator  $\mathbf{D}$  that approximate the first-order derivative in our problem is:

$$\mathbf{D} = 2\bar{\mathbf{D}}. \quad (43)$$

The beauty of the pseudo-spectral collocation method is that higher-order derivatives can be computed by computing the power of  $\mathbf{D}$ , that is, the  $i$ th order derivative can be approximated by  $\mathbf{D}^i$ . The discretized form of the boundary value problem is:

$$(1 + S)\mathbf{D}^2\mathbf{u} + Re\mathbf{D}\mathbf{u} - K(\mathbf{D}\mathbf{u})^2 \odot (\mathbf{D}\mathbf{u}) + P\mathbf{1} = 0,$$

$$\mathbf{D}^2\theta + Pe\mathbf{D}\theta + Br \left( (1 + S)(\mathbf{D}\mathbf{u})^2 - \frac{b}{6}(\mathbf{D}\mathbf{u})^4 \right) = 0, \quad (44)$$

$$\text{where } \mathbf{u} = \begin{bmatrix} u_1 \\ u_2 \\ \vdots \\ u_n \end{bmatrix}_{n \times n}, \quad \theta = \begin{bmatrix} \theta_1 \\ \theta_2 \\ \vdots \\ \theta_n \end{bmatrix}_{n \times n}, \quad \mathbf{1} = \begin{bmatrix} 1 \\ 1 \\ \vdots \\ 1 \end{bmatrix}_{n \times n}.$$

$u_i = u(\eta_i)$  and  $\theta_i = \theta(\eta_i)$ . The system of nonlinear equations in (44) can be written as:

$$\mathbf{F} = \begin{bmatrix} (1 + S)\mathbf{D}^2\mathbf{u} + Re\mathbf{D}\mathbf{u} - K(\mathbf{D}\mathbf{u})^2 \odot (\mathbf{D}\mathbf{u}) + P\mathbf{1} \\ \mathbf{D}^2\theta + Pe\mathbf{D}\theta + Br \left( (1 + S)(\mathbf{D}\mathbf{u})^2 - \frac{b}{6}(\mathbf{D}\mathbf{u})^4 \right) \end{bmatrix} = \begin{bmatrix} 0 \\ 0 \end{bmatrix}. \quad (45)$$

The boundary conditions can be imposed as:

$$F(1) = u(1), \quad (46)$$

$$F(n) = u(n), \quad (47)$$

$$F(n + 1) = \theta(1), \quad (48)$$

$$F(2n + 1) = \theta(n) - 1, \quad (49)$$

where  $u(1) = 0$  and  $u(n) = 0$ ,  $\theta(1) = 0$  and  $\theta(n) = 1$  describe the boundary conditions. The system of nonlinear equations (44) (after the adjustment of boundary conditions) can be solved by using the Newton method. The Newton method is used in the following form:

$$z_{k+1} = z_k - (\mathbf{F}'(z_k))^{-1}\mathbf{F}(z_k), \quad k = 0, 1, \dots \quad (50)$$

where  $z = [u, \theta]^T$ ,  $z_0 = 0$ , and  $F'(z_k)$  are the Jacobian of the system of nonlinear equations. We evaluate the Jacobian for the nonlinear system of equations and avoid the direct computation of Jacobian inverse for each iteration of Newton's method. To compute Jacobian's inverse at each iteration of Newton's method is computationally very expensive but gives us a quadratic convergence. To avoid the computation of Jacobian at each iteration, we freeze the Jacobian for some number of iterations (say for five iterations) and then periodically update it. The freezing of the Jacobian can compromise the quadratic convergence order. By running some simulations, one may find a trade-off between higher order of accuracy and low computational cost. The direct computation of Jacobian can be avoided by computing the LU-factors of Jacobian. We computed the LU-factors of the Jacobian and used them to solve the lower and upper triangular system of linear equations instead of computing the direct inverse. As we are



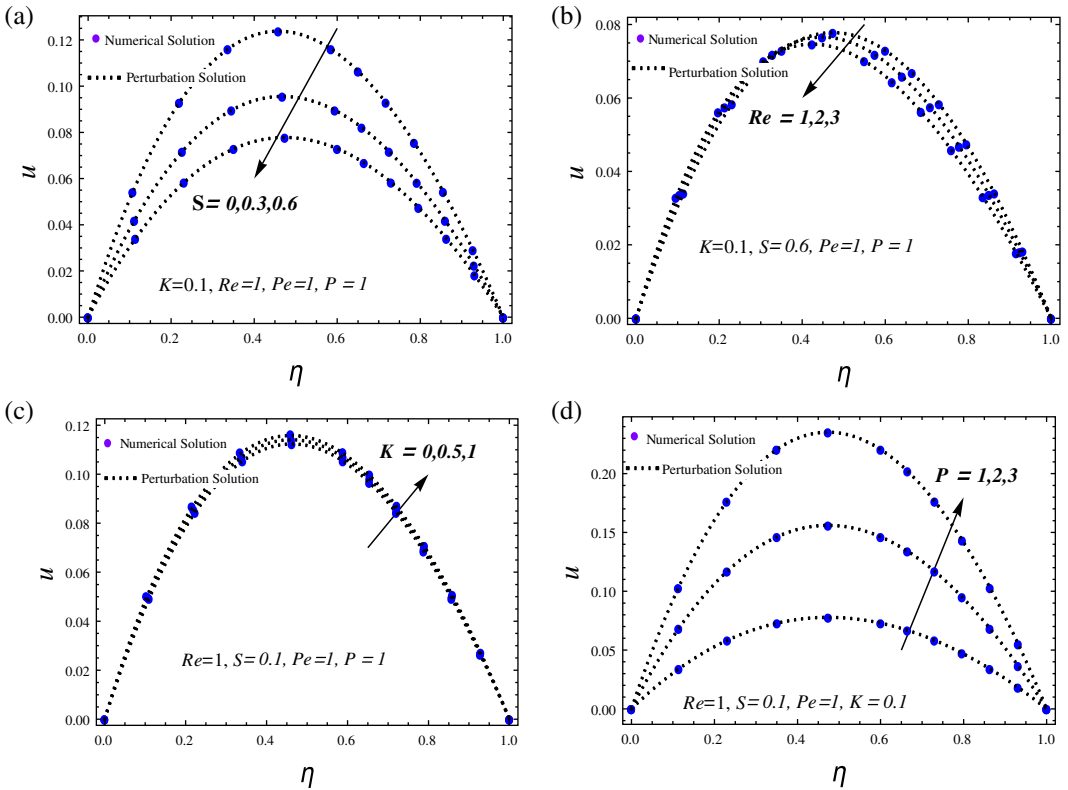


**FIGURE 2** Variation of velocity distribution [Color figure can be viewed at wileyonlinelibrary.com]

using the freezing-Jacobian strategy, we use the LU-factors repeatedly to fix the number of iterations. By using the technique of freezing Jacobian, we perform 10 iterations of Newton’s method on average to achieve 7-digits of accuracy in the numerical solution of the system of nonlinear equations. To perform numerical simulation, we take the size of the system of nonlinear equation  $n = 100$ . The total number of equations is 200; we are solving a system of nonlinear coupled equations. In all the simulations, we take  $\mathbf{0}$ , as an initial guess, and on average we get numerical accuracy in the solution of a system of nonlinear equations.

## 6 | RESULTS AND DISCUSSION

Non-Newtonian fluid such as an Eyring–Powell fluid with entropy generation inside an infinite pipe is considered here. The effects of various fluidic parameters on velocity and temperature profiles are highlighted through graphs and illustrated in Figures 2–7. The entropy generation number is also accounted for constants viscosity model. The analytical expressions of velocity, temperature, and entropy-generation numbers are obtained under the implementation of the perturbation technique. The range of parameters are: material parameter  $S$  is  $0 \leq S \leq 1$ , material parameter  $K$  ( $0 \leq K \leq 1$ ), material parameter  $b$  ( $0.1 \leq b \leq 3$ ), pressure number  $P$  ( $0 \leq P \leq 3$ ), Reynolds number  $Re$  ( $1 \leq Re \leq 5$ ), Peclet number  $Pe$  ( $1 \leq Pe \leq 5$ ), Brinkman number  $Br$  ( $0 \leq Br \leq 5$ ) and the value of temperature difference parameter  $\Omega$  is fixed 0.017 [34] for the construction of entropy generation number against the length of the channel.

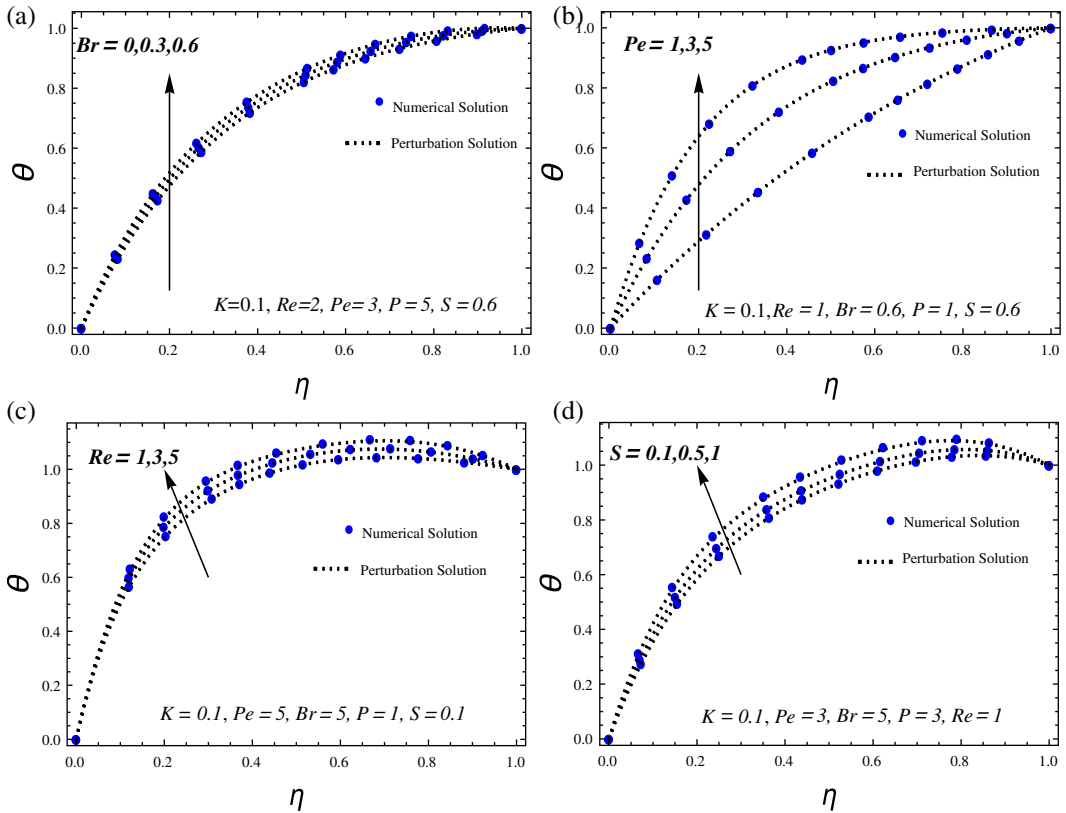


FIGURE 3 Variation of temperature distribution [Color figure can be viewed at [wileyonlinelibrary.com](http://wileyonlinelibrary.com)]

The effects of fluidic parameters such as Reynolds number ( $Re$ ), pressure parameter ( $P$ ), and material parameters  $S$  and  $K$  on velocity profiles are presented in Figure 2. The effects of  $S$  on the velocity profile are indicated in Figure 2a while the rest of the fluidic parameters are fixed. The velocity field decreases versus  $S$  throughout the channel. The reason is that for higher values of material parameter  $S$ , the viscosity of the fluid increases. Due to an increase in the viscosity of the fluid, the velocity profile is showing decreasing behavior. On the other hand, against the values of Reynolds number, the velocity profile is showing the increasing trend while the rest of the channel the opposite trend is noted via Reynolds number values (see Figure 2b). The velocity profiles increase with material parameter  $K$  and pressure parameter  $P$ . Generally, the velocity profile of an Eyring–Powell fluid is shows a parabolic trajectory. Furthermore, the velocity profile attains the maximum height in the center of the channel (see Figure 2c,d). The effects of pertinent parameters, namely, Brinkman number ( $Br$ ), Peclet number ( $Pe$ ), Reynolds number ( $Re$ ), and material parameter ( $S$ ) on temperature profile, are expressed in Figure 3. The temperature increases by increasing the values of Brinkman number ( $Br$ ) (Figure 3a). The reason is that the viscous dissipation effects increase the temperature of the fluid in the channel. It is observed that the temperature field has a direct relation with the Reynolds number, Peclet number, and material parameter (see Figure 3b–d). These parameters also increase the temperature of the fluid. Figure 4 exhibits the effects of emerging material parameters ( $S$  and  $b$ ), Brinkman number ( $Br$ ), and pressure parameter ( $P$ ) on entropy number ( $N_s$ ) against the length of the channel. The entropy generation number  $N_s$  is a decreasing function of material parameters

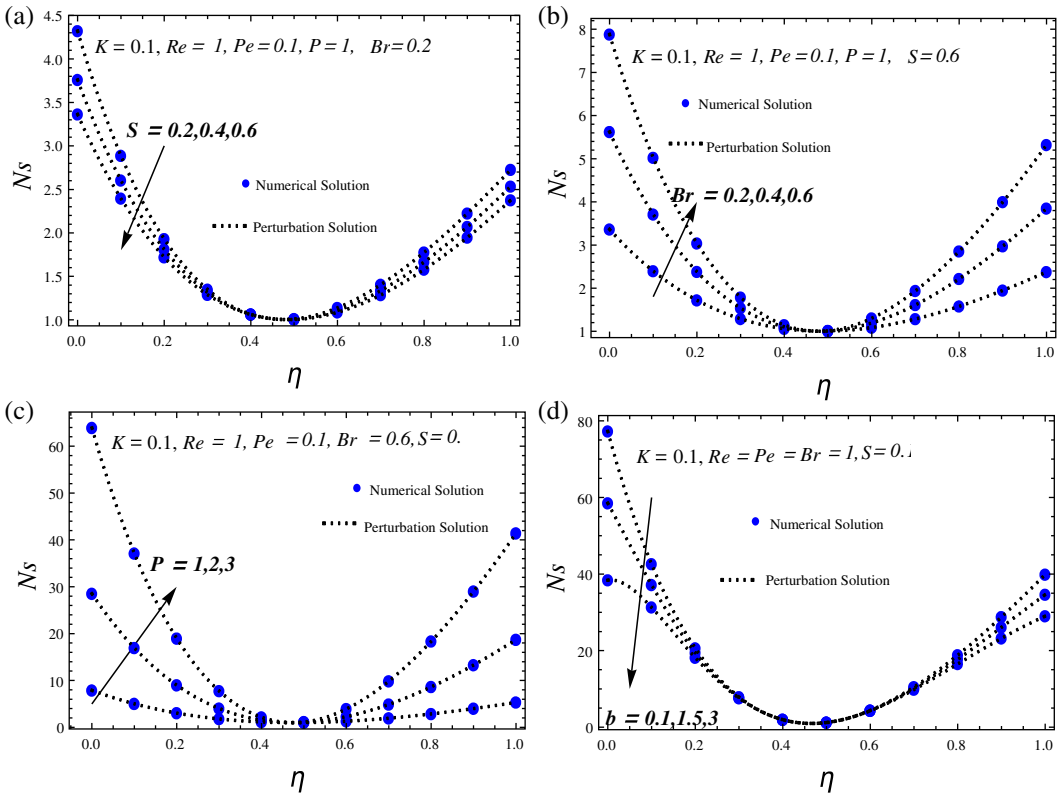


FIGURE 4 Variation of entropy generation distribution [Color figure can be viewed at wileyonlinelibrary.com]

$S$  and  $b$  while the reverse behavior is observed against Brinkman number  $Br$  and pressure parameter  $P$ . It is noted that the entropy number is maximum near the boundaries of the channel and decreases expressively as the center of the channel. The variation of Bejan number ( $Be$ ) against various fluidic parameters ( $Br$ ,  $Pe$ ,  $S$ , and  $K$ ) are plotted against the length of channel distance ( $\eta$ ) in Figure 5. The Bejan number is decreasing against Brinkman number and material parameter  $S$  and reverse behavior is noted against Peclet number and material parameter  $K$ . The magnitude of error between velocity and temperature distribution for Eyring–Powell fluid are also noted and plots in Figures 6 and 7, respectively. These figures show the order of accuracy in temperate and velocity profiles, which is of order  $10^{-6}$ .

## 7 | CONCLUSIONS

An approximate analytical solution for the computational study of non-Newtonian (Eyring–Powell) fluid under the impacts of Bejan and Entropy numbers in a porous channel is presented in this investigation. The analytical expressions of velocity, temperature, and entropy number are obtained by using the perturbation method. The effects of various pertinent parameters on velocity, temperature, entropy number are discussed. The analytical solution is compared with a numerical solution. For this, the pseudo-spectral method was used and the error plots of velocity and temperature profiles were constructed. The comparison of analytical and numerical solutions helped to confirm the validity of the

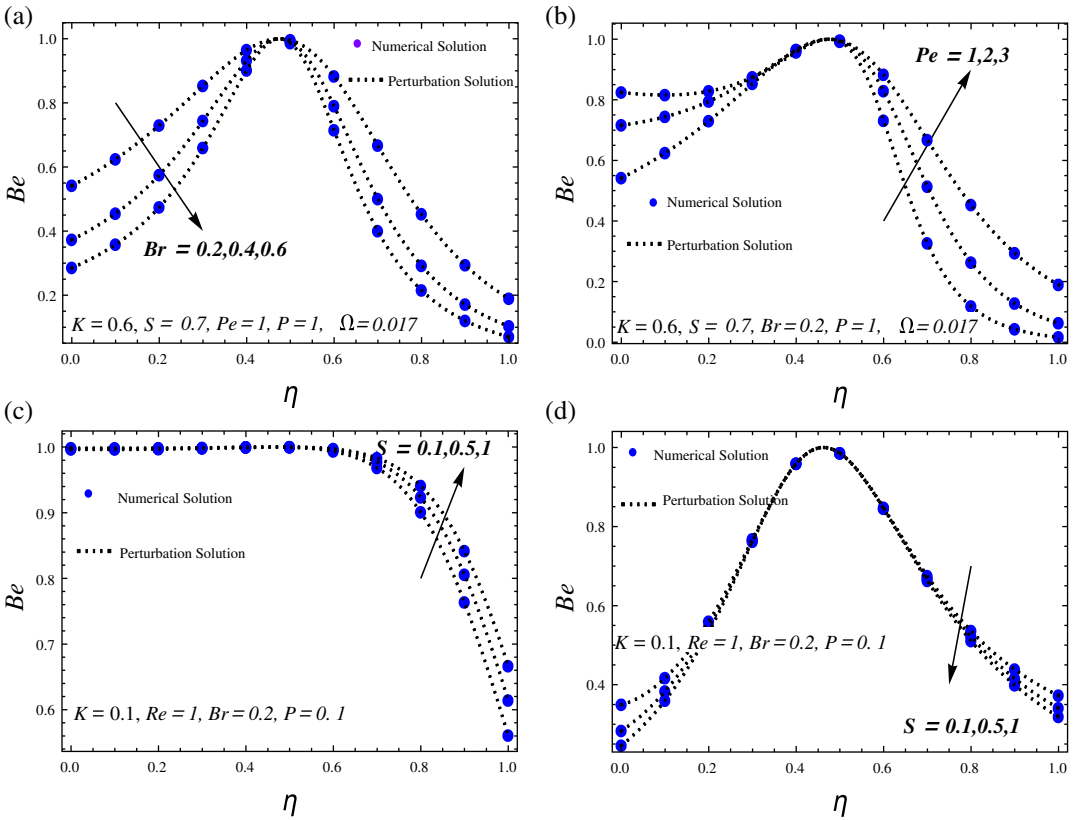


FIGURE 5 Variation of Bejan number [Color figure can be viewed at wileyonlinelibrary.com]

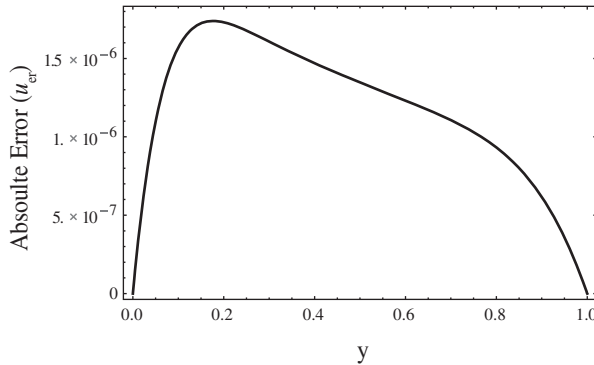


FIGURE 6 Absolute error in the velocity field

obtained results. A highly accurate method (pseudo spectral collocation method) is used to discretize the system of boundary value problems and finally, the Newton method which has quadratic convergence is employed to solve the associated system of nonlinear equations. On average,  $10^{-6}$  accuracy is obtained in the numerical results. The number of iterations was six to find the accuracy in temperature and velocity. These results will be validated with experimental data of Eyring–Powell fluid under the same assumptions in future work.

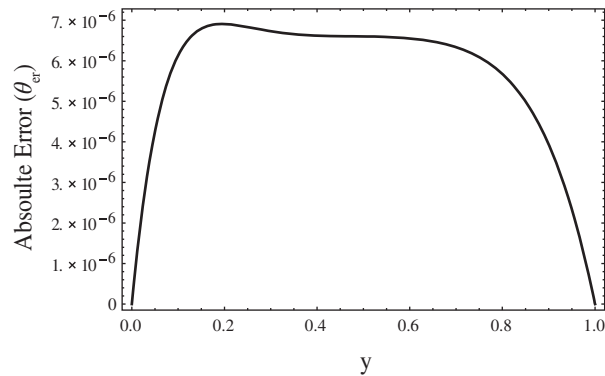


FIGURE 7 Absolute error in the temperature field

#### ACKNOWLEDGMENT

The research was supported by the National Natural Science Foundation of China (Grant Nos. 11971142, 11871202, 61673169, 11701176, 11626101, 11601485).

#### ORCID

Mubbashar Nazeer  <https://orcid.org/0000-0002-1657-4127>

Fayyaz Ahmad  <https://orcid.org/0000-0003-4372-3922>

Muhammad Ijaz Khan  <https://orcid.org/0000-0002-9041-3292>

#### REFERENCES

- [1] R. E. Powell and H. Eyring, *Mechanisms for the relaxation theory of viscosity*, Nature 154 (1944), 427–428.
- [2] B. S. Yilbas and M. Pakdemirli, *Entropy generation due to the flow of a non-Newtonian fluid with variable viscosity in a circular pipe*, J. Heat Transf. Eng. 26 (2011), 80–86.
- [3] M. Nazeer et al., *Natural convection through spherical particles of micropolar fluid enclosed in trapezoidal porous container: Impact of magnetic field and heated bottom wall*, Eur. Phys. J. Plus 133 (2018), 423.
- [4] M. Nazeer, N. Ali, and T. Javed, *Numerical simulation of MHD flow of micropolar fluid inside a porous inclined cavity with uniform and non-uniform heated bottom wall*, Can. J. Phys. 96 (2019), 576–593.
- [5] M. Nazeer, M. Ali, and T. Javed, *Natural convection flow of micropolar fluid inside a porous square conduit: Effects of magnetic field, heat generation/absorption and thermal radiation*, Journal of Porous Media. 21 (2018), 953–975.
- [6] M. Nazeer et al., *Numerical solution for flow of a Eyring–Powell fluid in a pipe with prescribed surface temperature*, J. Braz. Soc. Mech. Sci. Eng. 41 (2019), 518.
- [7] Z. Asghar et al., *An implicit finite difference analysis of magnetic swimmers propelling through non-Newtonian liquid in a complex wavy channel*, Comput. Math. Appl. 79 (2020), 2189–2202.
- [8] Z. Asghar et al., *Cilia-driven fluid flow in a curved channel: Effects of complex wave and porous medium*, Fluid Dyn. Res. 52 (2020), 015514.
- [9] Z. Asghar et al., *Bio-inspired propulsion of microswimmers within a passive cervix filled with couple stress mucus*, Comput. Methods Programs Biomed. 189 (2020), 105313.
- [10] Z. Asghar et al., *Locomotion of an efficient biomechanical sperm through viscoelastic medium*, Biomech. Model. Mechanobiol. (2020). <https://doi.org/10.1007/s10237-020-01338-z>.
- [11] M. Waqas, *A mathematical and computational framework for heat transfer analysis of ferromagnetic non-Newtonian liquid subjected to heterogeneous and homogeneous reactions*, J. Magnet. Mater. 493 (2020), 165646.
- [12] T. Hayat et al., *Numerical simulation for radiative flow of nanoliquid by rotating disk with carbon nanotubes and partial slip*, Comput. Methods Appl. Mechan. Eng. 341 (2018), 397–408.

- [13] M. Waqas, T. Hayat, and A. Alsaedi, *A theoretical analysis of SWCNT–MWCNT and H<sub>2</sub>O nanofluids considering Darcy–Forchheimer relation*, Appl. Nanosci. 9 (2019), 1183–1191.
- [14] N. Ali et al., *Buoyancy driven cavity flow of a micropolar fluid with variably heated bottom wall*, Heat Transf. Res. 49 (2018), 457–481.
- [15] N. Ali et al., *A numerical study of micropolar flow inside a lid-driven triangular enclosure*, Meccanica 53 (2018), 3279–3299.
- [16] G. H. R. Kefayati, *Thermosolutal natural convection of viscoplastic fluids in an open porous cavity*, Int. J. Heat Mass Transf. 138 (2019), 401–419.
- [17] G. H. R. Kefayati, *Simulation of double diffusive natural convection and entropy generation of power-law fluids in an inclined porous cavity with Soret and Dufour effects (part II: Entropy generation)*, Int. J. Heat Mass Transf. 94 (2016), 582–624.
- [18] M. A. Sheremet and I. Pop, *Mixed convection in a lid-driven square cavity filled by a nanofluid: Buongiorno's mathematical model*, Appl. Math. Comput. 266 (2015), 792–808.
- [19] M. Turkyilmazoglu, *Anomalous heat transfer enhancement by slip due to nanofluids in circular concentric pipes*, Int. J. Heat Mass Transf. 85 (2015), 609–614.
- [20] M. A. Sheremet, M. S. Astanina, and I. Pop, *MHD natural convection in a square porous cavity filled with a water-based magnetic fluid in the presence of geothermal viscosity*, Int. J. Numer. Methods Heat Fluid Flow 28 (2018), 2111–2131.
- [21] F. M. Elniel et al., *Approximate analytical solution of the MHD Powell–Eyring fluid flow near accelerated plate*, Malays. J. Fundam. Appl. Sci. 13 (2017), 416–420.
- [22] P. M. Krishna et al., *Dual solutions for unsteady flow of Powell–Eyring fluid past an inclined stretching sheet*, J. Naval Archit. Marine Eng. 13 (2016), 89–99.
- [23] S. O. Alharbi et al., *Entropy generation in MHD Eyring–Powell fluid flow over an unsteady oscillatory porous stretching surface under the impact of thermal radiation and heat source/sink*, J. Appl. Sci. 8 (2018), 1–18.
- [24] T. Javed et al., *Flow of an Eyring–Powell non-Newtonian fluid over a stretching sheet*, J. Chem. Eng. Commun. 200 (2013), 327–336.
- [25] M. Y. Malik et al., *Mixed convection flow of MHD Eyring–Powell nanofluid over a stretching sheet: A numerical study*, AIP Adv. 5 (2015), 1–13.
- [26] P. B. S. Kumar et al., *Mixed convection 3D radiating flow and mass transfer of Eyring–Powell nanofluid with convective boundary condition*, Defect Diffus. Forum 388 (2018), 158–170.
- [27] M. Nazeer et al., *Effects of constant and space-dependent viscosity on Eyring–Powell fluid in a pipe: Comparison of the perturbation and explicit finite difference methods*, Z. Naturforsch. A 74 (2019), 961–969.
- [28] F. Ahmad et al., *Heat and mass transfer of temperature-dependent viscosity models in a pipe: Effects of thermal radiation and heat generation*, Z. Naturforsch. A 75 (2020), 225–239.
- [29] N. Ali, F. Nazeer, and M. Nazeer, *Flow and heat transfer analysis of an Eyring–Powell fluid in a pipe*, Z. Naturforsch. A 73 (2018), 265–274.
- [30] T. Hayat, M. Zubair, M. Waqas, A. Alsaedi, and M. Ayub, *On doubly stratified chemically reactive flow of Powell–Eyring liquid subject to non-Fourier heat flux theory*, Results Phys., 7, 99–106 (2017).
- [31] T. Hayat et al., *Mixed convection stagnation-point flow of Powell–Eyring fluid with Newtonian heating, thermal radiation, and heat generation/absorption*, J. Aerospace Eng. 30 (2017), 04016077.
- [32] A. A. Khan, F. Zaib, and A. Zaman, *Effects of entropy generation on Powell–Eyring fluid in a porous channel*, J. Braz. Soc. Mech. Sci. Eng. 39 (2017), 5027–5036.
- [33] F. Ahmad, E. Tohidi, and J. A. Carrasco, *A parameterized multi-step Newton method for solving systems of nonlinear equations*, Numer. Algorithms 71 (2016), 631–653.
- [34] M. Pakdemirli and B. S. Yilbas, *Entropy generation for pipe flow of a third grade fluid with Vogel model viscosity*, Int. J. Non-Linear Mech. 41 (2006), 432–437.

**How to cite this article:** Nazeer M, Ahmad F, Ali W, et al. Perturbation and numerical solutions of non-Newtonian fluid bounded within in a porous channel: Applications of pseudo-spectral collocation method. *Numer Methods Partial Differential Eq.* 2020;1–15. <https://doi.org/10.1002/num.22613>

APPENDIX A.

$$\lambda_0 = \frac{-P}{Re},$$

$$\lambda_1 = \frac{Pe \frac{Re}{\Gamma}}{\left(-1 + e^{\frac{Re}{\Gamma}}\right) Re},$$

$$\lambda_2 = -\left( \frac{e^{-\frac{2Re}{\Gamma}} \left(1 + e^{\frac{Re}{\Gamma}}\right) \sigma Re^2 \lambda_1^3}{6\Gamma^3} + \frac{\sigma Re \lambda_0 \lambda_1 \left(\lambda_0 + \left(1 - e^{-\frac{Re}{\Gamma}}\right) \lambda_1\right)}{\left(-1 + e^{\frac{Re}{\Gamma}}\right) \Gamma^2} \right),$$

$$\lambda_3 = \frac{Re \lambda_0^2 \lambda_1}{\Gamma^2 \left(-1 + e^{\frac{Re}{\Gamma}}\right)}, \quad \lambda_4 = \frac{Re \lambda_0 \lambda_1^2}{\Gamma^2 \left(-1 + e^{\frac{Re}{\Gamma}}\right)}, \quad \lambda_5 = \frac{Re^2 \lambda_1^3}{6\Gamma^3 \left(-1 + e^{\frac{Re}{\Gamma}}\right)},$$

$$\chi_0 = \frac{e^{Pe}}{-1 + e^{Pe}}, \quad \chi_1 = -\frac{1}{Pe}, \quad \chi_2 = \frac{\lambda_0^2(-6\Gamma + b\lambda_0^2)}{6Pe}, \quad \chi_3 = \frac{2\lambda_0\Gamma(3\Gamma - b\lambda_0^2)\lambda_1}{3(Pe\Gamma - Re)},$$

$$\chi_4 = \frac{Re(\Gamma - b\lambda_0^2)\lambda_1^2}{2(Pe\Gamma - 2Re)}, \quad \chi_5 = -\frac{2bRe^2\lambda_0\lambda_1^3}{9\Gamma(Pe\Gamma - 3Re)}, \quad \chi_6 = -\frac{bRe^3\lambda_1^4}{24\Gamma^2(Pe\Gamma - 4Re)},$$

$$\chi_7 = \frac{e^{Pe} \left( \chi_2 + \left(-1 + e^{-\frac{Re}{\Gamma}}\right) \chi_3 - \chi_4 + e^{-\frac{2Re}{\Gamma}} \chi_4 - \chi_5 + e^{-\frac{3Re}{\Gamma}} \chi_5 - \chi_6 + e^{-\frac{4Re}{\Gamma}} \chi_6 \right)}{(-1 + e^{Pe})},$$

$$\chi_8 = \frac{\left( e^{Pe} \chi_2 - \chi_3 - \chi_4 - \chi_5 - \chi_6 + e^{Pe - \frac{4Re}{\Gamma}} \left( e^{\frac{3Re}{\Gamma}} \chi_3 + e^{\frac{2Re}{\Gamma}} \chi_4 + e^{\frac{Re}{\Gamma}} \chi_5 + \chi_6 \right) \right)}{1 - e^{Pe}},$$

$$\chi_9 = -\frac{Re\chi_3}{\Gamma}, \quad \chi_{10} = -\frac{2Re\chi_4}{\Gamma}, \quad \chi_{11} = -\frac{3Re\chi_5}{\Gamma}, \quad \chi_{12} = -\frac{4Re\chi_6}{\Gamma}, \quad \chi_{13} = -Pe\chi_7.$$